ACS OMEGA

http://pubs.acs.org/journal/acsodf

Article

Thermosensitive Injectable Chitosan/Collagen/β-Glycerophosphate Composite Hydrogels for Enhancing Wound Healing by Encapsulating Mesenchymal Stem Cell Spheroids

Ming Yang,* Shuohai He, Ziyue Su, Zihang Yang, Xinxin Liang, and Yingzhu Wu*

Cite This: *ACS Omega* 2020, 5, 21015−21023

Read Online

ACCESS | Metrics & More | Article Recommendations

ABSTRACT: Chronic wounds caused by diabetic or venous diseases remain a social and healthcare burden. In this work, a new strategy is proposed in which injectable thermosensitive chitosan/collagen/β-glycerophosphate (β-GP) hydrogels were combined with three-dimensional mesenchymal stem cell (3D MSC) spheroids to accelerate chronic wound healing by enhanced vascularization and paracrine effects. Chitosan/collagen/β-GP solution mixed with 3D MSC spheroids was rapidly transformed to a gel at body temperature by physical cross-linking, then overlapped the wounds fully and fitted to any shape of the wound. The results showed that the combination therapy exhibited a markedly therapeutic effect than the hydrogel-loaded two-dimensional (2D) MSCs or 2D MSCs alone. The hydrogel could provide an environment conductive to the attachment and proliferation of encapsulated MSCs, especially accelerating the proliferation and paracrine factor secretion of 3D MSC spheroids. These results supplied a novel alternative approach to treat chronic wounds caused by diabetic or venous diseases.

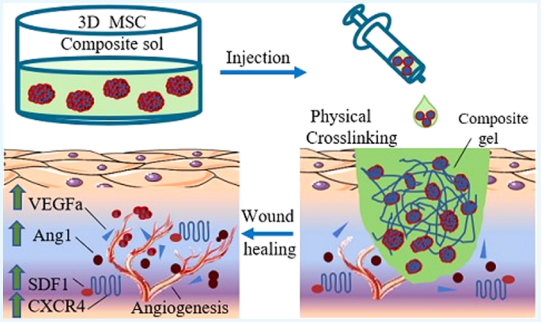

1. INTRODUCTION

Optimal wound healing is involved in a complex physiological process in which different types of cells participate and communicate with each other via diverse chemokines and cytokines, leading to cell proliferation, the generation of neovascularization and granulation tissue, and then epidermis formation.[1−4] However, chronic wounds caused by diabetes become hard to heal due to their compromised wound healing processes.[3,4] To date, typical treatment for chronic wounds includes the application of bioengineered artificial skin substitutes, topical delivery of an antioxidant, anti-inflammatory and antibacterial agents, and topical delivery of mesenchymal stem cells (MSCs) to speed up wound healing by decreasing inflammation, promoting angiogenesis, and decreasing scarring.[1,3−6] New research in wound healing comes from material science involving innovative material design. Therapy with the injectable natural biomaterials is attractive due to their biodegradability, biocompatibility, and minimally invasive implantation, such as chitosan[7−10] and type 1 collagen.[12,13] However, conventional thermogels usually suffer from poor physical properties and low cell-binding affinity, limiting their practical applications.[11,12] Materials fabricated with chitosan have received considerable attention for pharmaceutical and medical applications due to their promising properties,[8,10,13,14] such as antimicrobial activity, good biocompatibility, biodegradability, and good physical stability. Collagen is a major component of the extracellular matrix (ECM) in the dermal tissue and provides intrinsic cell-binding motifs and nanoarchitecture that assist in cell adhesion, migration, and proliferation.[15,16] A chitosan-mixed collagen hydrogel has been demonstrated as an efficient candidate for stem cell transplantation.[7,17,18] To enhance the mechanical properties, β-glycerophosphate (β-GP), an organic and nontoxic compound, has been used as a physical cross-linker in chitosan/collagen solution, which can cause a sol−gel transition at physiological pH and temperature.[18,19] Thermosensitive or pH-responsive gels can be applied to personalized/customized medical treatments and to tune the degradation time of implantable scaffolds or ingestible electronics.[18]

MSCs have been used to treat a wide range of diseases including lung injury, kidney disease, myocardial infarction, peripheral vascular disease, and diabetic wound.[6,20−22] The effects of two-dimensional (2D) MSC transplantation or chitosan hydrogels on wound healing showed good therapeutic efficacy.[6,10,23] Nevertheless, previous studies revealed that MSCs from conventional 2D culture condition have lots of disadvantages, including increased cell size, increased cellular

Received: June 1, 2020
Accepted: August 3, 2020
Published: August 12, 2020

senescence, decreased pluripotent gene expression such as *Nanog*, *Sox2*, and *Oct4*, reduced production of paracrine factors, and reduced capacity of engraftment and homing to injured tissues.[24,25] In comparison with 2D monolayer MSCs, three-dimensional (3D) MSC spheroids display superior therapeutic potential in the treatment of various diseases due to their enhanced capacity of multilineage differentiation, angiogenesis, anti-inflammatory effects, paracrine effects, prolonged in vivo retention, and higher expression of pluripotency markers.[26−29] However, the effects of the combination of 3D MSCs and natural biomaterials on wound healing are still not completely clear.

In the present study, we developed a novel therapeutic strategy based on an injectable chitosan/collagen/β-glycerophosphate hydrogel with a 3D MSC spheroid for improving MSC engraftment and directing cell function modification to accelerate wound healing in diabetic mouse models. 3D MSC aggregates/spheroids were formed at the bottom of the drop in short-term hanging-drop culture due to gravity. MSC spheroids were encapsulated by chitosan/collagen/β-GP solution; the mixtures were injected into the wound bed and changed from a liquid at room temperature to a gel at body temperature. Finally, the benefits of thermosensitive injectable chitosan/collagen/β-GP hydrogels embedded with 3D MSC spheroids to wound healing were evaluated and compared to the benefits of monolayer-cultured single cells directly dropped into the wound bed and of monolayer-cultured single cells encapsulated in the same carrier. The combination of a chitosan/collagen/β-GP hydrogel and 3D MSC spheroids on wound healing was reported for the first time, and the results indicated that the novel therapeutic strategy would be very promising in the treatment of chronic wounds caused by diabetic or venous diseases.

2. RESULTS

2.1. Formation and Characterization of 3D MSC Spheroids. The hanging-drop culture technique is a well-established method to establish spheroids from various types of cells. As shown in Figure 1a, 3D MSC spheroids were generated by pipetting a single-cell suspension onto the inner surface of a Petri dish lid. The cells were aggregated at the bottom of the droplet by gravity and surface tension, thereby forming the spheroids. 3D MSC spheroids cultured in such a way had a controlled cell number and spheroid size. As shown in Figure 1b,c,f, the 3D MSC spheroids showed size homogeneity during culture. Moreover, 3D MSC spheroids cultured for 36 and 60 h had no significant difference, with an average diameter of approximately 100 μm (Figure 1e). Then, the viability of the formed 3D MSC spheroids was assessed by staining with calcein-AM/ethidium homodimer-1 to visualize living (green) and dead (red) cells (Figure 1d). The result showed that 3D MSC spheroids exhibited great viability (>98%) using the presented hanging-drop method.

2.2. Superior Property of a Chitosan/Collagen/β-GP Hydrogel in the MSC Culture. The preparation of a chitosan/collagen/β-GP hydrogel was performed as described previously.[17] As shown in Figure 2a, chitosan/collagen/β-GP solution was liquid at room temperature but transformed to a solid gel after incubation at 37 °C. This thermal responsive property makes it easier for the cells to be mixed in the hydrogel at room temperature and then injected into the wound sites before gel formation in situ. Then, the biocompatibility of the chitosan/collagen/β-GP hydrogel was

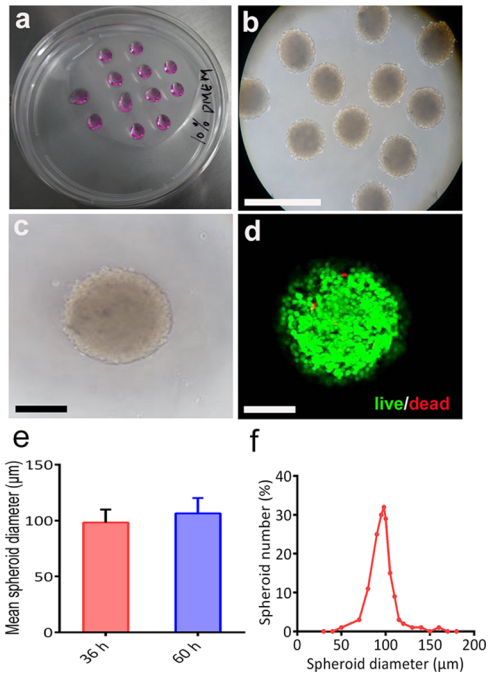

Figure 1. Formation of 3D MSC spheroids and cell viability. (a) Hanging-drop method. Hanging drops, each containing approximately 5000 cells, are deposited and grown under a 10 cm dish lid. (b, c) Morphology of 3D MSC spheroids with size homogeneity. (d) Representative live/dead image showing cell viability of a 3D MSC spheroid. 3D MSC spheroids were stained with calcein-AM/ethidium homodimer-1 to visualize living (green) and dead (red) cells (d). (e) MSC spheroid diameters after culture for 36 and 60 h were measured with a particle analyzer using Image J software (measurement of 200 spheroids each). (f) Size distribution of MSC spheroids cultured for 60 h is shown. Scale bar in (b) was 200 μm, scale bars in (c, d) were 50 μm.

determined in the MSC culture (Figure 2b,c). Minimal cytotoxicity, increased spreading, and proliferation were seen in MSC cultures with the chitosan/collagen/β-GP hydrogel. Most MSC grew well in the chitosan/collagen/β-GP hydrogel and rare dead cells were observed by live/dead kit staining assay. 2D monolayer MSC showed enhanced spreading in the chitosan/collagen/β-GP hydrogel (Figure 2b). 3D MSC exhibited increased cell numbers, and the cells from the periphery of 3D spheroids also spread and interacted with the hydrogel (Figure 2c). The cell proliferation rate was confirmed by DNA contents quantification, as shown in Figure 2d. The DNA content increased more evidently in 3D MSC spheroids than in 2D monolayer MSC when grown in the chitosan/collagen/β-GP hydrogel.

2.3. Effects of a 3D MSC Spheroid-Encapsulated Chitosan/Collagen/β-GP Hydrogel on Wound Healing in db/db Mice. An in vivo study was conducted on db/db diabetic mice on which two 6 mm full-thickness excisional skin wounds were created (Figure 3a). Murine excisional wound splinting was performed as described previously to delay the healing[33] and thus to allow a better evaluation of the healing effects of the novel therapeutic strategy. The wounds were treated, respectively, by an injection of 2D monolayer MSC without the hydrogel as a control, a 2D monolayer MSC-encapsulated chitosan/collagen/β-GP hydrogel and a 3D MSC spheroid-encapsulated chitosan/collagen/β-GP hydrogel and the results showed that the 3D MSC spheroid-encapsulated

https://dx.doi.org/10.1021/acsomega.0c02580
ACS Omega 2020, 5, 21015−21023

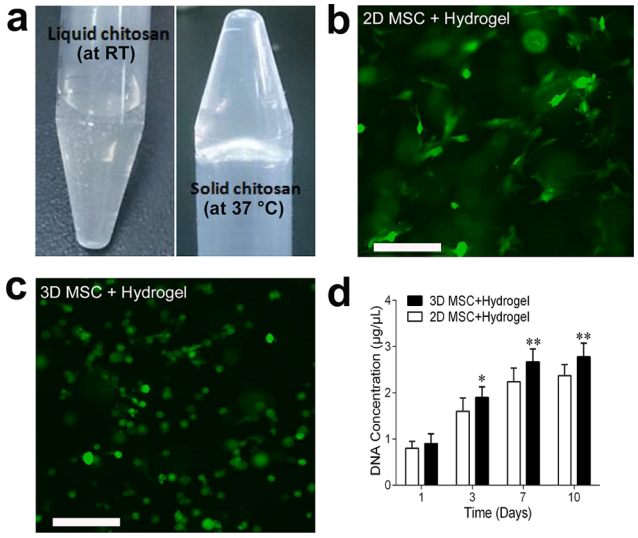

Figure 2. Thermosensitive property and cell proliferation in a 3D MSC spheroid-encapsulated chitosan/collagen/β-GP hydrogel. (a) Representative images of a chitosan/collagen/β-GP hydrogel showing thermosensitive property. The hydrogel changed from a liquid at room temperature (RT) to a gel at 37 °C. (b, c) Fluorescence microscopic images of calcein-AM staining of 2D MSC (b) and 3D MSC spheroids (c) encapsulated in a chitosan/collagen/β-GP hydrogel after 1 week of culture. Representative images are shown. Scale bar was 200 μm. (d) MSC proliferation in the hydrogel was determined by DNA content quantification at days 1, 3, 7, and 10. Experiments were performed in triplicate wells. Data are representative of three independent experiments (n = 3; *, P < 0.05; **, P < 0.01).

chitosan/collagen/β-GP hydrogel accelerated wound closure in db/db mice compared with the control group and the 2D monolayer MSC-encapsulated chitosan/collagen/β-GP hydrogel-treated group (Figure 3a). The enhancement appeared at 1 week after implantation and became more evident at week 2. At week 3, 10 of 14 wounds in 3D MSC spheroid-encapsulated chitosan/collagen/β-GP hydrogel-treated db/db mice (n = 7) achieved almost complete wound closure compared with the control group(n = 6) and the 2D monolayer MSC-encapsulated chitosan/collagen/β-GP hydrogel-treated group (n = 5). The areas of wound healing were measured on wound tissue samples from all tested mice at different time points and the variation of wound healing percentage was considered statistically significant among different treatments (p < 0.01). The results revealed that the total area of the wounds from the group treated with the 3D MSC spheroid-encapsulated chitosan/collagen/β-GP hydrogel decreased significantly with time compared with other two groups (Figure 3b).

The 3D MSC spheroid-encapsulated chitosan/collagen/β-GP hydrogel appeared to promote re-epithelialization of wounds in db/db diabetic mice (Figure 4a,b). The histological examination of wounds in db/db mice at 1 and 2 weeks revealed that the rates of re-epithelialization increased in 3D MSC spheroid-encapsulated chitosan/collagen/β-GP hydrogel-treated wounds (complete epithelialization in 13 of 14 wounds, n = 7) compared with the control group (complete epithelialization in 5 of 12 wounds, n = 6) or the 2D monolayer MSC-encapsulated chitosan/collagen/β-GP hydrogel-treated group (complete epithelialization in 6 of 10 wounds, n = 5). In accordance with the results from H&E staining (Figure 4a), the microphotographs of the wound bed (original magnification × 100) from the 3D MSC spheroid-encapsulated chitosan/collagen/β-GP hydrogel-treated group exhibited the increased re-epithelization velocity at 3 weeks and almost complete closure, but no completely re-epithelized and closed wounds were seen in other two groups (Figure 4b).

2.4. 3D MSC Spheroid-Encapsulated Chitosan/Collagen/β-GP Hydrogel Accelerated Wound Healing through Enhanced Vascularization and Paracrine Effects in Wounds. To confirm the effect of the 3D MSC spheroid-encapsulated chitosan/collagen/β-GP hydrogel on the vascularization of the wound bed in db/db mice, immunofluorescent staining of wound tissue at 2 weeks was performed. Immunofluorescent staining of wound samples for vascular endothelial antibody CD31 indicated increased microvessels in 3D MSC spheroid-encapsulated chitosan/

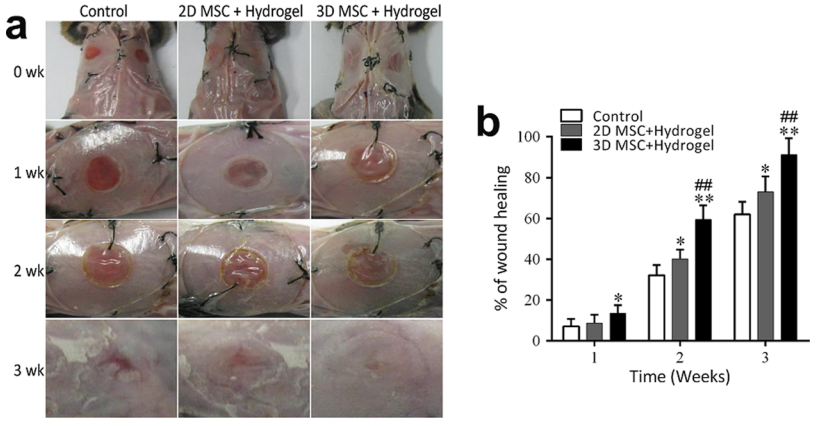

Figure 3. Wound-healing acceleration in 3D MSC spheroid-encapsulated chitosan/collagen/β-GP hydrogel-treated diabetic mice. (a) Representative images of the wound in db/db mice at week(s) 0, 1, 2, and 3. Murine excisional wound splintings (top panel) were created on the dorsal skin of db/db mice and the wound received implantation of 2D monolayer MSC without the hydrogel as a control, a 2D monolayer MSC-encapsulated chitosan/collagen/β-GP hydrogel, and a 3D MSC spheroid-encapsulated chitosan/collagen/β-GP hydrogel. The photographs of the first three panels were taken with transparent Tegaderm dressing, and those from the last panel were taken after removal of the dressing. (b) Wound closure areas were measured at week(s) 1, 2, and 3 in the control group (n = 12), the 2D MSC + hydrogel group (n = 10), and the 3D MSC + hydrogel group (n = 14). Analysis of variance (ANOVA): versus control, *, P < 0.05; **, P < 0.01; and versus 2D MSC + hydrogel group, ##, P < 0.01. Abbreviation: 2D, two-dimensional; 3D, three-dimensional; MSC, mesenchymal stem cells; wk, week(s).

https://dx.doi.org/10.1021/acsomega.0c02580
ACS Omega 2020, 5, 21015−21023

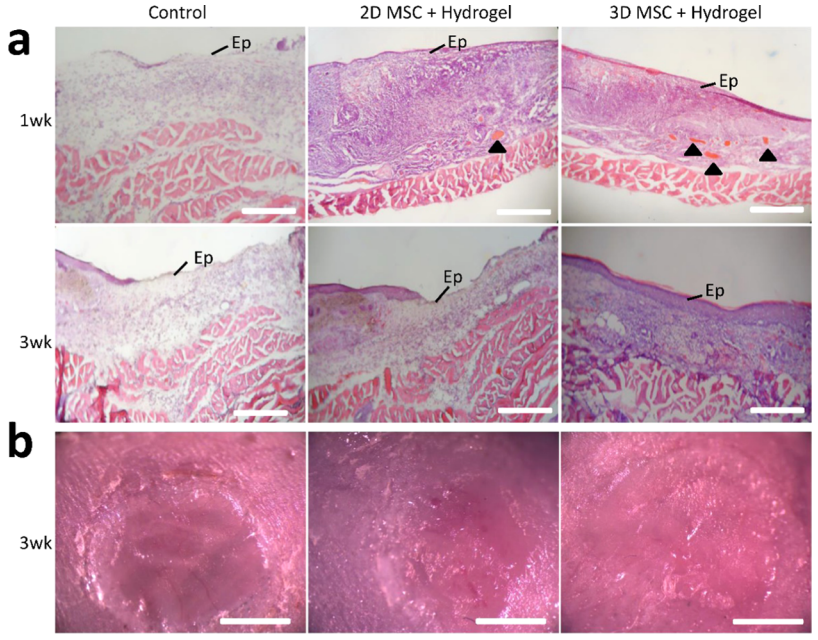

Figure 4. Histological examination of the wound tissue in diabetic mice at week(s) 1 and 3 after implantation. (a) Representative 1 week-wound or 3 week-wound tissue samples stained with hematoxylin and eosin (H&E). Black arrows show arterioles containing erythrocytes. Scale bar was 500 μm. (b) Microphotographs of the wound bed from different transplantation groups at week 3 show the rate of re-epithelization and closure in the wound. Scale bar was 2 mm. Abbreviations: Ep, epidermis, wk, week.

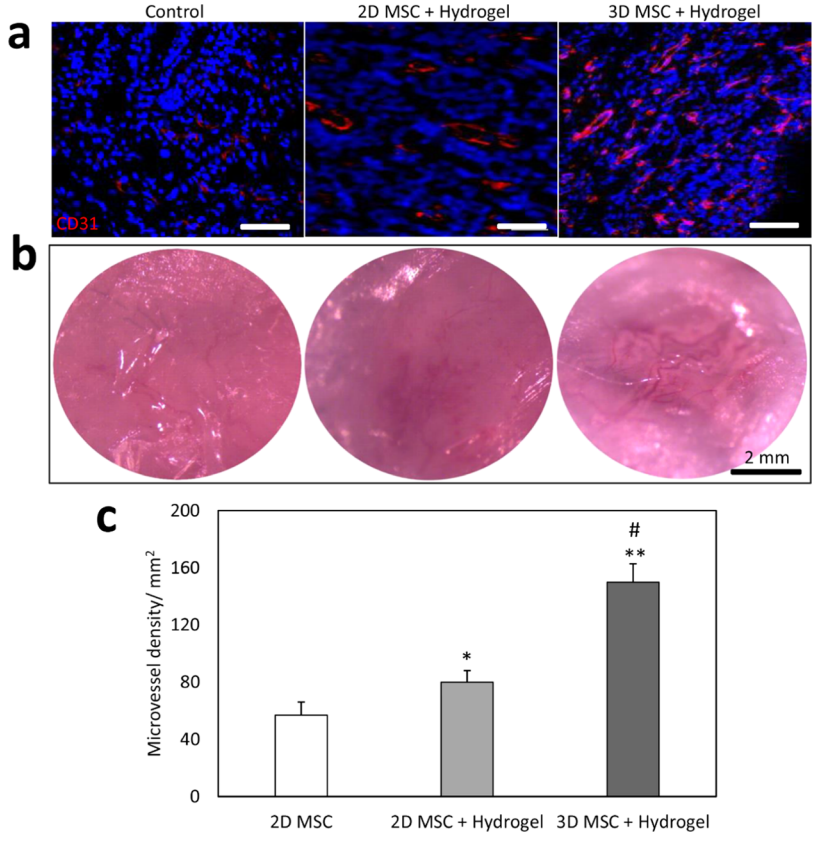

Figure 5. Effects of the 3D MSC spheroid-encapsulated chitosan/collagen/β-GP hydrogel on the vascularization in the wound. (a) Representative confocal images of wound tissue sections immunostained with a vascular endothelial antibody CD31 2 weeks after transplantation. Nuclei (blue) were stained with 4,6-diamidino-2-phenylindole (DAPI). Scale bar = 50 μm. (b) Micrograph of microvessels in the 2-week-old wound area. The microvessel density within the wound area (×200) is higher in the 3D MSC spheroid-encapsulated chitosan/collagen/β-GP hydrogel-treated group compared with other two groups. (c) Densities of microvessels in wounds were assessed morphometrically after immunostaining for CD31 (n = 8). Analysis of variance (ANOVA); versus control, *, $P < 0.05$; **, $P < 0.01$; and versus 2D MSC + hydrogel group, #, $P < 0.01$.

https://dx.doi.org/10.1021/acsomega.0c02580
ACS Omega 2020, 5, 21015−21023

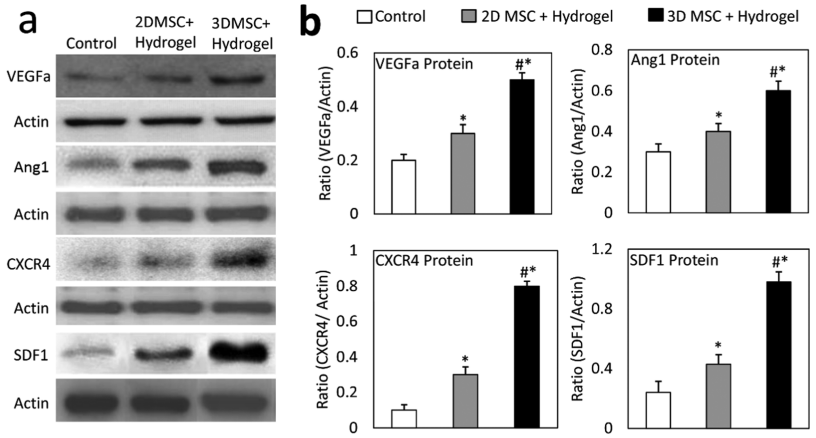

Figure 6. Expression of paracrine cytokines in wound tissues. The differential expression of VEGFa, Ang1, CXCR4, and SDF1 protein in 2D monolayer MSC-treated (control), 2D monolayer MSC-encapsulated chitosan/collagen/β-GP hydrogel-treated, and 3D MSC spheroid-encapsulated chitosan/collagen/β-GP hydrogel-treated wounds were detected by western blot assay (a) and quantified (b) after the first week of treatment. The experiment was repeated three times, and one representative result is shown. Analysis of variance (ANOVA), versus control, *, $P < 0.05$; and versus 2D MSC + hydrogel group, #, $P < 0.01$. Abbreviations: Ang, angiopoietin; VEGF, vascular endothelial growth factor.

collagen/β-GP hydrogel-treated wounds compared with other two treatment wounds (Figure 5a), which was consistent with the analysis of H&E staining (arterioles indicated with black arrows in Figure 4a). As shown in Figure 5b, numerous mature vessels were observed clearly around the wound bed, especially increased blood vessels and their branches presented in the 3D MSC spheroid-encapsulated chitosan/collagen/β-GP hydrogel-treated wounds. The microvessel densities in wounds at 2 weeks were analyzed morphometrically after immunofluorescent staining for CD31. The microvessel number per microphotograph (×100) in wound tissues was determined ($n = 7$) and microvessel densities within the wound area after 2 weeks of implantation were assessed, as shown in Figure 5c. The results showed that there was a moderate increase in the number of microvessels in wounds treated with the 2D MSC-encapsulated hydrogel compared to local 2D MSC alone injection (57 ± 9.11 vs $80 \pm 8.13/mm^2$, $p < 0.05$), but neovascularization was further augmented in wounds treated with the 3D MSC-encapsulated hydrogel compared to the 2D MSC-encapsulated hydrogel ($150 \pm 12.78/mm^2$ vs $80 \pm 8.13/mm^2$, $p < 0.01$). Our results demonstrated that the 3D MSC spheroid-encapsulated chitosan/collagen/β-GP hydrogel contributed to wound closure by accelerating angiogenesis under the local wound environment.

To determine whether the 3D MSC spheroid-encapsulated chitosan/collagen/β-GP hydrogel could enhance wound healing through a paracrine effect, we performed western blot analysis of wound tissue samples at 1 week after implantation. Our data showed that angiogenesis factors VEGFa and Ang-1 were expressed much higher in the wounds treated with the 3D MSC spheroid-encapsulated chitosan/collagen/β-GP hydrogel, which were almost 3-fold or 1.5-fold greater than those in the control group or the 2D monolayer MSC-encapsulated chitosan/collagen/β-GP hydrogel-treated group, respectively (Figure 6a,b). CXCR4 and SDF-1 were demonstrated to be more important in the enhanced therapeutic effects in many diseases due to their enhanced migration capacity.[30] So, they had also been detected in this study and the results showed that CXCR4 and SDF1 protein expression levels significantly increased in 3D MSC spheroid-encapsulated chitosan/collagen/β-GP hydrogel-treated wounds; CXCR4 and SDF1 protein presented 2.7-, and 2.3-fold change, respectively, compared with 2D MSC-encapsulated chitosan/collagen/β-GP hydrogel-treated wounds (Figure 6a,b).

3. DISCUSSION

In recent years, great attention has been focused on the development of injectable therapeutic hydrogel biomaterials for skin wounds and tissue engineering.[12,17,31,32] In this study, we applied injectable thermosensitive chitosan/collagen/β-GP hydrogel, which are easy to use, especially for irregularly surfaced wounds due to in situ gel-forming ability at physiological temperature. In cell-based therapies, chitosan/collagen-based hydrogels provide an ECM like microenvironment and have good biocompatibility as well as biodegradability and are good cell carriers. The presence of collagen in the hydrogel has been proved to play an important role in mediating cell adhesion, migration, survival, and proliferation, as well as promoted gel remodeling due to its favorable chemical, physical, and biological characteristics.[15,16,18] Nowadays, chitosan scaffolds combined with collagen have received considerable attention in wound healing and skin engineering, partly owing to its low immunogenicity, specific recognition and interaction with cells, proper porous structure, and robust mechanical properties.[7,16−18] Herein, we combined the chitosan/collagen/β-GP hydrogel with 3D MSC spheroids and found that the chitosan/collagen/β-GP hydrogel exerted an enhanced effect on the proliferation and paracrine factor secretion of 3D MSC spheroids, which then contribute to its therapeutic effectiveness in full-thickness cutaneous wound healing through enhanced angiogenesis and re-epithelization.

The treatment of local wounds with MSC applications has gained popularity in recent years as a promising approach for the enhancement of tissue regeneration.[20−22,33] However, because of the harsh environment of the wound, the topical transplantation of MSCs alone onto the wound site exhibited poor postimplant cell survival, low engraftment efficiency, and limited cell retention.[34,35] A cell-encapsulated hydrogel was thought to be an effective means for improving stem cell therapeutic efficiency on wound regeneration, possibly by retaining injected cells at the site of administration for longer without a runoff.[12,17] In this study, we encapsulated 2D MSCs in the chitosan/collagen/β-GP hydrogel and found that the

https://dx.doi.org/10.1021/acsomega.0c02580
ACS Omega 2020, 5, 21015−21023

transplantation of 2D MSCs encapsulated in the chitosan/collagen/β-GP hydrogel significantly promoted wound healing as compared to transplantation of 2D MSC alone. Our results suggested that the chitosan/collagen/β-GP hydrogel could provide an appropriate environment for living cells while preventing their migration away from the targeted administration site due to its physiological pH and in situ gel-forming ability at physiological temperature.[12,17] Consistent with our findings, biomaterials consisting of chitosan exhibited great superiority in open wound healing in multiple animal models by enhancing the angiogenic activity of implanted MSCs, promoting granulation tissue formation and re-epithelialization.[12−14]

To further determine whether a 3D MSC spheroid-hydrogel combination wound increase healing efficacy, mice treated with a 2D MSC-loaded hydrogel or 3D MSC spheroid-loaded hydrogel were implemented in our study. Our data show that the administration of the 3D MSC-loaded chitosan/collagen/β-GP hydrogel displayed enhanced wound healing compared with that treated with the 2D MSC-loaded chitosan/collagen/β-GP hydrogel, suggesting that 3D MSC spheroids exert enhanced cellular activities and desirable wound repair microenvironment under the same housing conditions as compared with 2D MSC. In previous studies, it was found that the formation of MSC spheroids displayed enhanced proliferation, differentiation, migration potential, and increased cytokine release,[25,26,28,36] which was important for MSCs on wound healing. Consistent with our study, the combination of bone marrow-derived MSCs with the pullulan−collagen hydrogel showed significant promotion of wound closure by localization of cells within wounds, enhanced cell viability, and neovascularization, as well as enhanced stemness and regeneration.[37] In addition, the combination of the Pluronic F-127 hydrogel and Wharton's jelly mesenchymal stem cells has been shown to have enhanced wound healing potential through potential M2 macrophage formation and enhanced angiogenesis.[38] Murphy et al. demonstrated that the MSC spheroid-encapsulated fibrin hydrogel accelerated wound healing by enhanced secretion of bioactive factors to promote neovascularization and modulate the inflammatory milieu.[39] These results and ours suggested that combination therapy can provide a potential way for chronic wound treatment with high quality.

In our findings, 3D MSC exhibited increased cell numbers, and the cells from the periphery of 3D spheroids also spread and interacted with the hydrogel when embedded in the chitosan/collagen/β-GP hydrogel after being cultured for one week, which probably attributed to the fact that 3D culture can maintain the stemness, decrease cellular senescence, and enhance the self-renewal capacity of MSC.[26,29,36] In addition, the hydrogel provided a suitable microenvironment, like ECM, for transplanted stem cell adhesion and survival.[12,37] Therefore, 3D MSC spheroids displayed rapid cell proliferation and stimulated tissue remodeling via physical or chemical cues when embedded in the chitosan/collagen/β-GP hydrogel.

Paracrine signaling from MSCs is considered the primary mechanism through which these cells reduce inflammation, promote angiogenesis, and tissue remodeling in the wound.[5,21] In previous literature, it was found that the paracrine effects were enhanced when MSCs were cultured as spheroids.[28,29,36,40] Our current study demonstrated that the transplantation of 3D MSC spheroids encapsulated in the chitosan/collagen/β-GP hydrogel promotes more paracrine cytokine secretion in the wounds compared with that treated with the 2D MSC-loaded chitosan/collagen/β-GP hydrogel or 2D monolayer MSC alone. Angiogenesis factors VEGFa, Ang-1 were significantly increased at the protein expression level in the wounds treated with the 3D MSC-chitosan/collagen/β-GP hydrogel. VEGFa and Ang-1 were reported to stimulate endothelial cell proliferation and promote endothelial tube formation in vitro and in vivo.[5,21] CXCR4 and SDF-1 were demonstrated to be more important in the enhanced therapeutic effects in many diseases due to their enhanced migration capacity and recruiting endothelial cells into injury sites.[5,30] CXCR4 is the receptor of SDF1, which was chemotactic and released postinjury to recruit cells for neovascularization.[30] Therefore, the increased expression of SDF1 and CXCR4 in wounds treated with the 3D MSC-chitosan/collagen/β-GP hydrogel found in this study may implicate enhanced migration and homing of MSCs, leading to accelerated re-epithelialization and angiogenesis. The formation of microvessels plays a very important role in sustaining the newly formed granulation tissues in the wound and supporting keratinocyte survival.[6,41] BM-MSC was demonstrated to promote wound healing in diabetic mice through enhanced neovascularization.[6,20,28] In this study, a significant increase of blood vessel density at the wound area at 2 weeks after transplantation of the 3D MSC-chitosan/collagen/β-GP hydrogel indicated remarkable neovascularization by the increased release of paracrine factors. Our data suggested that the chitosan/collagen/β-GP hydrogel may act as a desirable carrier for enhancing 3D MSC functions and the cellular processes of healing. More interesting, biomaterials consisted of chitosan have been shown to have antimicrobial activity, wound-healing properties coupled with enhanced paracrine secretion.[7−10] The topical application of chitosan has been reported to promote the various phases of wound repair and then trigger the wound healing by inducing the extracellular matrix to facilitate cellular activities.[10,13,14]

Taken together, the combined efficiency suggested the chitosan/collagen/β-GP hydrogel as an efficient structural support to assist 3D MSC adhesion, survival, and proliferation in the wound, contributing to enhanced paracrine factor secretion, which results in accelerated re-epithelialization and angiogenesis.

4. CONCLUSIONS

In conclusion, these results illuminated the positive effect of an injectable thermosensitive chitosan/collagen/β-GP hydrogel in combination with 3D MSC spheroids on wound healing in diabetic mice. The hydrogel-3D MSCs combination therapy exhibited a markedly therapeutic effect than the hydrogel-loaded 2D MSCs or 2D MSCs alone. The hydrogel could provide an environment conductive to the attachment and proliferation of encapsulated MSCs, especially accelerating the proliferation and paracrine factor secretion of 3D MSC spheroids. The combined treatment accelerated the wound closure in diabetic mice by enhanced vascularization and paracrine effects. These results supplied a novel alternative approach to treat chronic wounds caused by diabetic or venous diseases. However, this work has limitations; the mechanisms of enhanced efficiency of 3D MSC hydrogel-combined treatment for chronic wound has not been fully investigated, the mechanotransduction, interactions of 3D MSC spheroids with the hydrogel, and detailed signaling pathway need to be clarified in future work.

https://dx.doi.org/10.1021/acsomega.0c02580
ACS Omega 2020, 5, 21015−21023

5. EXPERIMENTAL SECTION

5.1. Isolation and Culture of Human Placental MSCs. Human placenta-derived MSCs were isolated and cultivated as described previously.[42] Briefly, term (38−40 weeks gestation) placentas from three healthy donors were collected after acquiring written informed consent. All procedures were approved by the Ethics Committee of Xili Hospital. The placental tissues were washed several times with precooled saline solutions and then minced and trypsinized at 37 °C for 30 min in a water bath. The samples were subsequently prepared in both single-cell suspensions and small digested residues by filtering, pelleting, and resuspending procedures. Finally, they were encapsulated on uncoated polystyrene dishes and cultured with a growth medium consisting of Dulbecco's-modified Eagle's medium (DMEM, Gibco-Invitrogen, Carlsbad, CA), 10% fetal bovine serum (FBS; Gibco-Invitrogen), 100 U/mL penicillin, and 100 μg/mL streptomycin (Invitrogen, Paisley, U.K.). All cultures were maintained at 37 °C in a humidified atmosphere supplied with 5% CO_2. The culture medium was replaced every 2 days and cells were subcultured after trypsinization when they reached 80% confluence.

5.2. 3D MSC Spheroid Culture. hMSCs of passages 5−7 were used to create 3D spheroids by a hanging drop method.[43] Briefly, placental hMSCs grown as a monolayer were dissociated with 0.25% trypsin-ethylenediaminetetraacetic acid (EDTA) solution, collected by centrifugation, and then resuspended in a free-serum medium. These cells were encapsulated onto the lid of a Petri dish with 5000 cells/25 μL each droplet. The bottom of the dish was supplemented with 10 mL of phosphate-buffered saline (PBS) to avoid complete drying during culture. After 36 h of hanging up, they were transferred to a new noncoated culture plate and incubated in a fresh free-serum medium supplemented with 20 ng/mL bFGF, 20 ng/mL EGF, 25 ng/mL PDGF-BB, and B27 supplement (2%, Invitrogen) for 24 h. The spheroids were rotated gently every 6 h during suspension culture. These samples were used in the subsequent experiments.

5.3. Confocal Imaging of 3D Spheroids and Spheroid Viability Analysis. For confocal imaging, 3D MSC spheroids were stained with fluorescent markers.[44] Briefly, 3D MSC spheroids were washed gently two to three times with phosphate-buffered saline (PBS). Then, they were incubated in PBS containing 2 μM calcein-AM and 4 μM ethidium homodimer-1(LIVE/DEAD Kit, Life Technologies) for 2 h at 4 °C followed by 30 min at 37 °C to ensure enhanced staining of the interior of the spheroid. Following staining, the spheroids were washed with PBS and then used for confocal imaging with a Leica TCS SP2 confocal microscope. Spheroid images were constructed by creating a maximum projection of multiple z-plane sections spaced 3−7 μm apart. The proportion of living cells within a spheroid was evaluated by counting the number of live (green) and dead (red) cells in five different, equally spaced z-planes throughout the spheroid. ImageJ (*V*1.51*t*, National Institutes of Health, Bethesda, MD) was used for spheroid viability analyses.

5.4. Preparation of Chitosan/Collagen/β-Glycerophosphate Composite Hydrogel-Encapsulated MSC Spheroids. The fabrication of a composite hydrogel consisted of chitosan, collagen, and β-glycerophosphate (β-GP) was performed according to a method previously described.[18] Briefly, 1.7 wt % completely dissolved chitosan stock solutions were prepared by stirring autoclaved chitosan powder in 0.1 M hydrochloric acid for 18 h and stored at 4 °C. A sterile β-GP stock solution (56 wt %) was obtained after dissolution in deionized water and passed through a 0.22 μm filter membrane. Before use, the chitosan and collagen (Sigma, 4 mg/mL) solutions were mixed and stirred on the ice at a mass ratio of 2:1. Then, the precooled β-GP was added dropwise to the chitosan/collagen mixture with stirring on ice and its pH was adjusted to 7.0−7.2.

5.5. Cell Viability Analysis in the Hydrogel. Monolayer MSCs or MSC spheroids were encapsulated at a density of 1.0×10^6 cells/mL in the prepared chitosan/collagen/β-GP liquid solutions. The mixed solution was then transferred to a 24-well plate in a 37 °C incubator for gelation. After 8 min, each well was supplemented with 1 mL of the complete medium and continued to culture. The medium was changed every 2 days. Cell viability at day 1 and 7 was assessed using 2 μM calcein-AM and 4 μM ethidium homodimer-1(LIVE/DEAD Kit, Life Technologies). The cellular growth in the hydrogel was imaged by a Leica TCS SP2 confocal microscope.

5.6. DNA Content Quantification Assay in the Hydrogel. The cell number in the chitosan/collagen/hydrogel was assessed at 1, 3, 7, and 10 days through fluorometric quantification of the amount of cellular DNA following the manufacturer's instructions (PicoGreen dsDNA Quantitation kit, Invitrogen). Briefly, a cell-encapsulated hydrogel was suspended in Na citrate buffer solution containing 50 mM Na citrate and 100 mM NaCl and stored at −80 °C until use. After thawing, the cells were lysed to release DNA. The samples were centrifuged at 10 000*g* for 10 min to remove debris, and the extract was used for the PicoGreen assay according to the manufacturer's protocol. Ten microliters of cell lysates or DNA standards were mixed with 100 μL of 1× PicoGreen reagents and then used for fluorescence measurements at 560/590 nm (excitation/emission). The fluorescence of negative, cell-free controls was subtracted from the fluorescence values of the experimental groups to account for the background fluorescence. A standard curve based on the known DNA concentration was applied to determine the total cell DNA contents of the samples.

5.7. In Vivo MSC Transplantation Experiment. DB/DB mice (13 weeks old; female; body weight, 43.1 ± 2.6 g) were purchased from Jackson Laboratory. The animals were randomly divided into three groups. The excisional wound-splinting model was established as described previously.[6] First, two 6 mm full-thickness excisional skin wounds were created on each side of the midline of the dorsal skin after hair removal and anesthesia. Each wound received 1.0×10^6 cells from the monolayer or 3D spheroids encapsulated in 80 μL of the hydrogel. As the control group, the equal numbers of single cells were dropped into the wound bed directly without being embedded in the hydrogel. Then, the donut-shaped silicone splint was placed and fixed on the skin by the adhesive and interrupted sutures. Finally, Tegaderm (3M, London, ON, Canada) was placed over the wound to avoid contamination. The animals were housed individually and observed at week(s) 0, 1, 2, and 3.

5.8. Histologic Examination. Tissue samples were washed with precooled PBS and then were fixed with 3% paraformaldehyde at 4 °C for at least 24 h. The frozen tissues embedded in optimal cutting temperature (OCT) compounds were cut serially with a thickness of 10 μ and then stained with hematoxylin and eosin for light microscopy.

https://dx.doi.org/10.1021/acsomega.0c02580
ACS Omega 2020, 5, 21015−21023

5.9. Western Blotting. Western blotting was performed as described previously.[6] In brief, tissue protein samples were extracted in a lysis buffer consisted of 1% Triton X-100 and proteinase inhibitors (Sigma-Aldrich). Equal amounts of total protein (30 μg) were separated by 12% sodium dodecyl sulfate-polyacrylamide gel electrophoresis (SDS-PAGE) and transferred to nitrocellulose membranes. Membranes were blocked with 5% milk and then incubated overnight at 4 °C with a monoclonal antibody against Ang-1, Ang-2 (Chemicon, Temecula, CA), or VEGF-α (R&D Systems).

5.10. Immunofluorescence. For the analysis of the vascular density, tissue sections were permeabilized with 0.1% Triton X-100 for 10 min at room temperature. After being blocked with 5% bovine serum albumin (BSA), the sections were incubated with a primary antibody against endothelial cell markers CD31 (Sigma-Aldrich) overnight at 4 °C, followed by fluorescence-conjugated secondary antibodies. Nuclei were stained with 4,6-diamidino-2-phenylindole (DAPI). After mounting, the samples were visualized under a confocal microscope (FV1000; Olympus, Tokyo, Japan). Image J was used to binarize immunofluorescent images taken with the same excitation, gain, and exposure settings. Intensity threshold values were set automatically and the quantification of CD31 staining was determined by a pixel-positive area normalized to a dermal area.

5.11. Statistical Analysis. All data are expressed as mean ± standard deviation (SD). Student's paired t test was performed for the comparison of data of paired samples, and one-way ANOVA was used to analyze statistical differences between individual groups. A probability (p) value of <0.05 was considered statistically significant.

AUTHOR INFORMATION

Corresponding Authors

Ming Yang − *X&Y Industrial Company Limited, Shenzhen 518103, Guangdong, China*; Phone: 86 755 27806543; Email: 65552262@qq.com; Fax: 86 755 27806543

Yingzhu Wu − *School of Textile Materials and Engineering, Wuyi University, Jiangmen 529020, P. R. China.*; orcid.org/0000-0001-6861-5966; Phone: 86 750 3296060; Email: wuyingzhu111@163.com; Fax: 86 750 3296066

Authors

Shuohai He − *School of Textile Materials and Engineering, Wuyi University, Jiangmen 529020, P. R. China.*

Ziyue Su − *School of Textile Materials and Engineering, Wuyi University, Jiangmen 529020, P. R. China.*

Zihang Yang − *School of Textile Materials and Engineering, Wuyi University, Jiangmen 529020, P. R. China.*

Xinxin Liang − *School of Textile Materials and Engineering, Wuyi University, Jiangmen 529020, P. R. China.*

Complete contact information is available at: https://pubs.acs.org/10.1021/acsomega.0c02580

Notes

The authors declare no competing financial interest.

ACKNOWLEDGMENTS

This work was supported by the Guangdong Province Special Innovation Project (2017KTSCX182).

REFERENCES

(1) Shaw, T. J.; Martin, P. Wound repair at a glance. *J. Cell Sci.* **2009**, *122*, 3209−3213.

(2) Singer, A. J.; Clark, R. A. Cutaneous wound healing. *N. Engl. J. Med.* **1999**, *341*, 738−746.

(3) Falanga, V. Wound healing and its impairment in the diabetic foot. *Lancet* **2005**, *366*, 1736−1743.

(4) Martin, P.; Nunan, R. Cellular and molecular mechanisms of repair in acute and chronic wound healing. *Br. J. Dermatol.* **2015**, *173*, 370−378.

(5) Arno, A. I.; Amini-Nik, S.; Blit, P. H.; Al-Shehab, M.; Belo, C.; Herer, E.; Tien, C. H.; Jeschke, M. G. Human Wharton's jelly mesenchymal stem cells promote skin wound healing through paracrine signaling. *Stem Cell Res. Ther.* **2014**, *5*, 28.

(6) Wu, Y.; Chen, L.; Scott, P. G.; Tredget, E. E. Mesenchymal stem cells enhance wound healing through differentiation and angiogenesis. *Stem Cells* **2007**, *25*, 2648−2659.

(7) Wang, L.; Rao, R. R.; Stegemann, J. P. Delivery of mesenchymal stem cells in chitosan/collagen microbeads for orthopedic tissue repair. *Cells Tissues Organs* **2013**, *197*, 333−343.

(8) Kim, I. Y.; Seo, S. J.; Moon, H. S.; Yoo, M. K.; Park, I. Y.; Kim, B. C.; Cho, C. S. Chitosan and its derivatives for tissue engineering applications. *Biotechnol. Adv.* **2008**, *26*, 1−21.

(9) Zhu, M.; Liu, P.; Shi, H. G.; Tian, Y.; Ju, X. Y.; Jiang, S. D.; Li, Z.; Wu, M.; Niu, Z. W. Balancing antimicrobial activity with biological safety: bifunctional chitosan derivative for the repair of wounds with Gram-positive bacterial infections. *J. Mater. Chem. B* **2018**, *6*, 3884−3893.

(10) Bakshi, P. S.; Selvakumar, D.; Kadirvelu, K.; Kumar, N. S. Chitosan as an environment friendly biomaterial - a review on recent modifications and applications. *Int. J. Biol. Macromol.* **2020**, *150*, 1072−1083.

(11) Kim, B. S.; Cho, C. S. Injectable Hydrogels for Regenerative Medicine. *Tissue Eng. Regener. Med.* **2018**, *15*, 511−512.

(12) Nicodemus, G. D.; Bryant, S. J. Cell encapsulation in biodegradable hydrogels for tissue engineering applications. *Tissue Eng., Part B* **2008**, *14*, 149−165.

(13) Chi, J.; Zhang, X.; Chen, C.; Shao, C.; Zhao, Y.; Wang, Y. Antibacterial and angiogenic chitosan microneedle array patch for promoting wound healing. *Bioact. Mater.* **2020**, *5*, 253−259.

(14) Miguel, S. P.; Moreira, A. F.; Correia, I. J. Chitosan based-asymmetric membranes for wound healing: A review. *Int. J. Biol. Macromol.* **2019**, *127*, 460−475.

(15) Glowacki, J.; Mizuno, S. Collagen scaffolds for tissue engineering. *Biopolymers* **2008**, *89*, 338−344.

(16) Lin, K. L.; Zhang, D. W.; Macedo, M. H.; Cui, W. G.; Sarmento, B.; Shen, G. F. Advanced Collagen-Based Biomaterials for Regenerative Biomedicine. *Adv. Funct. Mater.* **2019**, *29*, No. 1804943.

(17) Shan, J.; Tang, B.; Liu, L.; Sun, X. B.; Shi, W.; Yuan, T.; Liang, J.; Fan, Y. J.; Zhang, X. D. Development of chitosan/glycerophosphate/collagen thermo-sensitive hydrogel for endoscopic treatment of mucosectomy-induced ulcer. *Mater. Sci. Eng., C* **2019**, *103*, No. 109870.

(18) Wang, L.; Stegemann, J. P. Thermogelling chitosan and collagen composite hydrogels initiated with beta-glycerophosphate for bone tissue engineering. *Biomaterials* **2010**, *31*, 3976−3985.

(19) Cho, J.; Heuzey, M. C.; Begin, A.; Carreau, P. J. Physical gelation of chitosan in the presence of beta-glycerophosphate: the effect of temperature. *Biomacromolecules* **2005**, *6*, 3267−3275.

(20) Guo, J. M.; Hu, H. D.; Gorecka, J.; Bai, H. L.; He, H.; Assi, R.; Isaji, T.; Wang, T.; Setia, O.; Lopes, L.; Gu, Y. Q.; Dardik, A. Adipose-derived mesenchymal stem cells accelerate diabetic wound healing in a similar fashion as bone marrow-derived cells. *Am. J. Physiol.: Cell Physiol.* **2018**, *315*, C885−C896.

(21) Li, J. Y.; Ren, K. K.; Zhang, W. J.; Xiao, L.; Wu, H. Y.; Liu, Q. Y.; Ding, T.; Zhang, X. C.; Nie, W. J.; Ke, Y.; Deng, K. Y.; Liu, Q. W.; Xin, H. B. Human amniotic mesenchymal stem cells and their paracrine factors promote wound healing by inhibiting heat stress-induced skin cell apoptosis and enhancing their proliferation through

activating PI3K/AKT signaling pathway. *Stem Cell Res. Ther.* **2019**, *10*, No. 247.
(22) Yue, C.; Guo, Z.; Luo, Y. F.; Yuan, J. J.; Wan, X. X.; Mo, Z. H. c-Jun Overexpression Accelerates Wound Healing in Diabetic Rats by Human Umbilical Cord-Derived Mesenchymal Stem Cells. *Stem Cells Int.* **2020**, *2020*, No. 7430968.
(23) El Sadik, A. O.; El Ghamrawy, T. A.; Abd El-Galil, T. I. The Effect of Mesenchymal Stem Cells and Chitosan Gel on Full Thickness Skin Wound Healing in Albino Rats: Histological, Immunohistochemical and Fluorescent Study. *PLoS One* **2015**, *10*, No. e0137544.
(24) Li, Z.; Liu, C. X.; Xie, Z. H.; Song, P. Y.; Zhao, R.CH.; Guo, L.; Liu, Z. G.; Wu, Y. J. Epigenetic Dysregulation in Mesenchymal Stem Cell Aging and Spontaneous Differentiation. *PLoS One* **2011**, *6*, No. e20526.
(25) Guo, L.; Zhou, Y.; Wang, S.; Wu, Y. J. Epigenetic changes of mesenchymal stem cells in three-dimensional (3D) spheroids. *J. Cell Mol. Med.* **2014**, *18*, 2009−2019.
(26) Baraniak, P. R.; McDevitt, T. C. Scaffold-free culture of mesenchymal stem cell spheroids in suspension preserves multilineage potential. *Cell Tissue Res.* **2012**, *347*, 701−711.
(27) Bartosh, T. J.; Ylostalo, J. H.; Bazhanov, N.; Kuhlman, J.; Prockop, D. J. Dynamic compaction of human mesenchymal stem/precursor cells into spheres self-activates caspase-dependent IL1 signaling to enhance secretion of modulators of inflammation and immunity (PGE2, TSG6, and STC1). *Stem Cells* **2013**, *31*, 2443−2456.
(28) Bhang, S. H.; Lee, S.; Shin, J. Y.; Lee, T. J.; Kim, B. S. Transplantation of cord blood mesenchymal stem cells as spheroids enhances vascularization. *Tissue Eng., Part A* **2012**, *18*, 2138−2147.
(29) Li, Y.; Guo, G.; Li, L.; Chen, F.; Bao, J.; Shi, Y. J.; Bu, H. Three-dimensional spheroid culture of human umbilical cord mesenchymal stem cells promotes cell yield and stemness maintenance. *Cell Tissue Res.* **2015**, *360*, 297−307.
(30) Wang, X. Y.; Jiang, B.; Sun, H. Y.; Zheng, D. J.; Zhang, Z. W.; Yan, L.; Li, E. Q.; Wu, Y. J.; Xu, R. H. Noninvasive application of mesenchymal stem cell spheres derived from hESC accelerates wound healing in a CXCL12-CXCR4 axis-dependent manner. *Theranostics* **2019**, *9*, 6112−6128.
(31) Cao, J.; Wang, P.; Liu, Y.; Zhu, C.; Fan, D. Double crosslinked HLC-CCS hydrogel tissue engineering scaffold for skin wound healing. *Int. J. Biol. Macromol.* **2020**, *155*, 625−635.
(32) Song, K. D.; Li, L. Y.; Yan, X. Y.; Zhang, W.; Zhang, Y.; Wang, Y. W.; Liu, T. Q. Characterization of human adipose tissue-derived stem cells in vitro culture and in vivo differentiation in a temperature-sensitive chitosan/beta-glycerophosphate/collagen hybrid hydrogel. *Mater. Sci. Eng., C* **2017**, *70*, 231−240.
(33) Maharlooei, M. K.; Bagheri, M.; Solhjou, Z.; Jahromi, B. M.; Akrami, M.; Rohani, L.; Monabati, A.; Noorafshan, A.; Omrani, G. R. Adipose tissue derived mesenchymal stem cell (AD-MSC) promotes skin wound healing in diabetic rats. *Diabetes Res. Clin. Pract.* **2011**, *93*, 228−234.
(34) Chen, J. S.; Wong, V. W.; Gurtner, G. C. Therapeutic potential of bone marrow-derived mesenchymal stem cells for cutaneous wound healing. *Front. Immunol.* **2012**, *3*, 192.
(35) Chen, L.; Tredget, E. E.; Liu, C.; Wu, Y. Analysis of allogenicity of mesenchymal stem cells in engraftment and wound healing in mice. *PLoS One* **2009**, *4*, No. e7119.
(36) Cheng, N. C.; Chen, S. Y.; Li, J. R.; Young, T. H. Short-term spheroid formation enhances the regenerative capacity of adipose-derived stem cells by promoting stemness, angiogenesis, and chemotaxis. *Stem Cells Transl. Med.* **2013**, *2*, 584−594.
(37) Rustad, K. C.; Wong, V. W.; Sorkin, M.; Glotzbach, J. P.; Major, M. R.; Rajadas, J.; Longaker, M. T.; Gurtner, G. C. Enhancement of mesenchymal stem cell angiogenic capacity and stemness by a biomimetic hydrogel scaffold. *Biomaterials* **2012**, *33*, 80−90.
(38) Deng, Q.; Huang, S.; Wen, J.; Jiao, Y.; Su, X.; Shi, G.; Huang, J. PF-127 hydrogel plus sodium ascorbyl phosphate improves Wharton's jelly mesenchymal stem cell-mediated skin wound healing in mice. *Stem Cell Res. Ther.* **2020**, *11*, No. 143.
(39) Murphy, K. C.; Whitehead, J.; Zhou, D.; Ho, S. S.; Leach, J. K. Engineering fibrin hydrogels to promote the wound healing potential of mesenchymal stem cell spheroids. *Acta Biomater.* **2017**, *64*, 176−186.
(40) Ryu, N. E.; Lee, S. H.; Park, H. Spheroid Culture System Methods and Applications for Mesenchymal Stem Cells. *Cells* **2019**, *8*, 1620.
(41) Shou, K.; Niu, Y.; Zheng, X.; Ma, Z.; Jian, C.; Qi, B.; Hu, X.; Yu, A. Enhancement of Bone-Marrow-Derived Mesenchymal Stem Cell Angiogenic Capacity by NPWT for a Combinatorial Therapy to Promote Wound Healing with Large Defect. *Biomed. Res. Int.* **2017**, *2017*, No. 7920265.
(42) Fukuchi, Y.; Nakajima, H.; Sugiyama, D.; Hirose, I.; Kitamura, T.; Tsuji, K. Human placenta-derived cells have mesenchymal stem/progenitor cell potential. *Stem Cells* **2004**, *22*, 649−658.
(43) Xu, F.; Sridharan, B.; Wang, S.; Gurkan, U. A.; Syverud, B.; Demirci, U. Embryonic stem cell bioprinting for uniform and controlled size embryoid body formation. *Biomicrofluidics* **2011**, *5*, 22207.
(44) Aijian, A. P.; Garrell, R. L. Digital microfluidics for automated hanging drop cell spheroid culture. *J. Lab. Autom.* **2015**, *20*, 283−295.

https://dx.doi.org/10.1021/acsomega.0c02580
ACS Omega 2020, 5, 21015−21023